

discussed the use of a multigap model in connection with $\epsilon(\omega)$. He finds that it is possible to give a

modestly good account of the optical properties in terms of gaps similar to the ones used here.

*Work performed under the auspices of the U.S. Atomic Energy Commission.

¹N. Wiser, Phys. Rev. 129, 62 (1963).

²H. Ehrenreich and M. H. Cohen, Phys. Rev. 115, 786 (1959).

³J. Lindhard, Kgl. Danske Videnskab. Selskab, Mat.-Fys. Medd. 28, 8 (1954).

⁴D. R. Penn, Phys. Rev. 128, 2093 (1962).

⁵G. Srinivasan, Phys. Rev. 178, 1245 (1969).

⁶J. C. Phillips, Rev. Mod. Phys. 42, 317 (1970).

⁷J. A. Van Vechten, Phys. Rev. 182, 891 (1969).

⁸H. Nara, J. Phys. Soc. Japan 20, 779 (1965); 20, 1097 (1965).

⁹J. P. Walter and M. L. Cohen, Phys. Rev. B 2, 1821 (1970).

¹⁰D. Brust, Solid State Commun. 9, 481 (1971).

¹¹D. Brust, J. Phys. C 4, L278 (1971).

¹²S. Groves and W. Paul, Phys. Rev. Letters 11, 194 (1963).

¹³L. Liu and D. Brust, Phys. Rev. Letters 20, 651 (1968).

¹⁴L. Liu and D. Brust, Phys. Rev. 173, 777 (1968).

¹⁵L. Liu and E. Tosatti, Phys. Rev. Letters 23, 772 (1969).

¹⁶J. G. Broerman, Phys. Rev. Letters 25, 1658 (1970).

¹⁷V. Heine and R. C. Jones, J. Phys. C 2, 719 (1969).

¹⁸D. Brust, Phys. Rev. 134, A1337 (1964).

¹⁹V. Heine and I. Abarenkov, Phil. Mag. 9, 451 (1964).

²⁰J. Hubbard, Proc. Roy. Soc. (London) A276, 238 (1964).

²¹M. Cardona, lecture notes (unpublished).

Temperature Dependence of the Optical Transmission Edge in $\text{Cd}_3(\text{As}_x\text{P}_{1-x})_2$ Alloys

P. L. Radoff and S. G. Bishop

Naval Research Laboratory, Washington, D.C. 20390

(Received 14 May 1971)

The temperature dependence of the transmission edge has been studied in several alloys of the $\text{Cd}_3(\text{As}_x\text{P}_{1-x})_2$ system for $0 \leq x \leq 1$. Analysis of the data on the basis of the Kane model suggests that a band crossover occurs near the Cd_3As_2 end of the system. An approximately linear variation is obtained for the energy gap E_g between interacting bands from 0.59 eV in Cd_3P_2 to -0.25 eV in Cd_3As_2 at helium temperatures. The temperature coefficient of the gap also shows a nearly linear variation from -3×10^{-4} eV/°K in Cd_3P_2 to -6×10^{-4} eV/°K in Cd_3As_2 for temperatures above 100 °K.

I. INTRODUCTION

The semiconducting alloys of the $\text{Cd}_3(\text{As}_x\text{P}_{1-x})_2$ system are of considerable practical importance, as well as of intrinsic interest, because of their relatively high mobilities, small effective masses, and optical gaps which vary with composition from 0.6 eV (for $x=0$) to less than 0.2 eV (for $x=1$) at low temperatures.¹⁻³ The alloys can be produced for all x , although for $x \leq 0.25$ Bridgman-grown ingots show cracks associated with the solid-solid phase transition which has been reported by several workers.^{3,4} Similar problems occur in Bridgman-grown Cd_3As_2 .

Most of the previous work on this system has centered on the end-point compounds Cd_3P_2 and Cd_3As_2 , which have been successfully grown by vapor deposition. Optically pumped coherent laser oscillations have been observed⁵ in as-grown Cd_3P_2 at a wavelength of 2.1 μ . In addition, when compensated, Cd_3P_2 is a sensitive low-temperature photoconductive detector with a 2- μ long-wavelength

cutoff.² Low-temperature photoluminescence and optical transmission studies have indicated a direct minimum gap near 0.6 eV.¹

At the other end of the system, room-temperature optical studies on thin films of Cd_3As_2 have been reported by Zdanowicz,⁶ who observed two absorption edges at about 0.14 and 0.6 eV. The lower-energy edge was attributed to indirect (Burstein-Moss-shifted) transitions from the valence band to the lowest conduction band, and the higher-energy edge to direct transitions to a remote conduction band. It was found that the effective mass of Cd_3As_2 , as determined from magnetoplasma studies,⁷ increases with temperature from about 0.041 m_0 at helium temperatures to 0.045 m_0 at room temperature. Shubnikov-de Haas (SdH) measurements³ have shown that the low-temperature effective mass also increases with carrier concentration and that the conduction band consists of a single, nearly spherical surface. The SdH data were analyzed by means of a nonparabolic model and yielded a value of 22 eV for E_p , the energy associated with the momen-

tum matrix element p (in Kane's formulation⁹). However, a substantially lower value of E_p (18–19 eV) was obtained from transport measurements at both nitrogen¹⁰ and room temperatures.¹¹

The most comprehensive work on the system as a whole is that of Wagner, Palik, and Swiggard,³ who reported measurements of room-temperature optical transmission and low-temperature interband magnetoabsorption (IMO) on several alloys. The IMO data were also analyzed on the Kane model and suggested that a band crossing takes place near the Cd_3As_2 end of the system. Thus, although it has often been assumed to be a positive-gap semiconductor,^{6,10,12} Wagner *et al.* concluded that Cd_3As_2 is a zero-gap material, much like HgTe ¹³ or $\alpha\text{-Sn}$.¹⁴ They fitted the earlier data of Haidemenakis *et al.*⁷ with a negative Kane gap of about -0.22 eV and obtained for E_p a value of about 15 eV, which is lower than any of the preceding results.^{8,10,11} On the other hand, theoretical work by Lin-Chung,¹⁵ based on a hypothetical model of the Cd_3As_2 crystal structure, resulted in a small positive energy gap for Cd_3As_2 , but did not entirely rule out the possibility of a zero-gap structure. This calculation also located the valence-band maxima away from the Γ point, although the minimum of the conduction band was fixed at Γ .¹⁶ The study of the temperature dependence of luminescence in the alloys¹⁷ tended to confirm the latter conclusion, but it was not possible to confirm or refute the validity of the band-crossing model.

The present study of the temperature dependence of the transmission edge was designed to characterize further the alloys of the $\text{Cd}_3(\text{As}_x\text{P}_{1-x})_2$ system. As shown below, these measurements can also be used to provide a confirmation of one or the other of the band models which have been proposed, in spite of the complications caused by the large numbers of free carriers ($\sim 10^{18}$ cm^{-3}). In particular, the low-temperature measurements can be compared directly with IMO results.³

In Sec. II of this paper the details of experimental apparatus are discussed. The results of measurement are presented and analyzed in Sec. III, and conclusions which can be drawn from these results are discussed in Sec. IV.

II. EXPERIMENTAL

The temperature dependence of the transmission edge in $\text{Cd}_3(\text{As}_x\text{P}_{1-x})_2$ reported here was studied in several unoriented single crystals, grown in our laboratory, with seven distinct values of x between 0 and 1. Six of the samples were cut from Bridgman ingots. Of the two as-grown Cd_3P_2 samples studied, one was vapor deposited and one was Bridgman grown. There were no substantial differences in the characteristics of these two samples. A third Cd_3P_2 sample was made by copper-doping a vapor-deposited sample. The Cd_3As_2 sample was

also vapor deposited. All alloy compositions except the (nominally) $x=0.12$ and the $x=0.35$ samples were determined with the use of standard chemical techniques; the values thus obtained were quite precisely those expected from the relative values of the constituents before growth.

The characteristics of the samples studied are shown in Table I. The as-grown samples were degenerate and had n -type carrier concentrations between 2×10^{17} and 2×10^{18} cm^{-3} which were nearly temperature independent. Copper doping is an effective means of compensating Cd_3P_2 .^{2,18} Thus the carrier concentration of the copper-doped sample at room temperature was about 10^{15} cm^{-3} (n type) and dropped sharply at low temperatures. The availability of this sample made possible the experimental determination of the Burstein-Moss shift of the energy gap for Cd_3P_2 at low temperatures.

The samples were glued to CaF_2 or Si substrates and polished to thicknesses between 50 and 100 μ . The substrates were then glued to a cold finger mounted on a cryostat whose temperature could be raised from 8 to 300 °K.

A tungsten lamp and a globar were used as sources over the spectral range 1.5–10 μ . The transmitted light was analyzed by a Perkin-Elmer model 210 grating monochromator and detected with a room-temperature PbS cell, a 78 °K InSb photo-voltaic cell, or a 78 °K $\text{Hg}_{0.76}\text{Cd}_{0.22}\text{Te}$ photoconductive detector, depending on the wavelength. The sample temperature was monitored by means of a Au (0.07 at. % Fe) Chromel thermocouple soldered to the cold finger. Absolute temperatures could be measured in this way to within 3 °K.

The optical transmission edge was arbitrarily defined from straight-line extrapolation of the linear portion of the transmission onset to zero transmission.³ The edges thus determined occur at wavelengths corresponding to absorption constants of about 300 cm^{-1} in as-grown Cd_3P_2 and about 1000 cm^{-1} in copper-doped Cd_3P_2 . The values of the edges thus obtained at the lowest temperature differ by about 25 meV—which corresponds to the calcu-

TABLE I. Room-temperature carrier density and Hall mobility, and low-temperature bottom-of-the-band mass for the $\text{Cd}_3(\text{As}_x\text{P}_{1-x})_2$ alloy samples studied.

Alloy	Carrier density (300 °K) N (cm^{-3})	Mobility (300 °K) μ ($\text{cm}^2/\text{V sec}$)	Bottom-of-the- band mass ($\sim 8^\circ\text{K}$) m_0^*/m_0
Cd_3P_2 (copper doped)	$\sim 10^{15}$		0.047
Cd_3P_2 (as grown)	2×10^{17}	1700	0.047
$\text{Cd}_3(\text{As}_{0.12}\text{P}_{0.88})_2$	6.3×10^{17}		0.039
$\text{Cd}_3(\text{As}_{0.25}\text{P}_{0.75})_2$	6.5×10^{17}	3800	0.021
$\text{Cd}_3(\text{As}_{0.35}\text{P}_{0.65})_2$	6.1×10^{17}	5600	0.016
$\text{Cd}_3(\text{As}_{0.50}\text{P}_{0.50})_2$	1.3×10^{18}	6100	0.009
$\text{Cd}_3(\text{As}_{0.75}\text{P}_{0.25})_2$	1.8×10^{18}	9500	0.002
Cd_3As_2	2×10^{18}	12800	0.014

lated difference in Fermi levels. In the case of Cd_3As_2 as well, the extrapolated edges agree accurately with previous absorption-constant determinations of the edge at two temperatures.¹² Hence the extrapolation technique provides a sufficiently accurate and useful means of defining the transmission edge.

III. RESULTS AND ANALYSIS

A. Energy Gap at Low Temperature

The compositional dependence of the low-temperature transmission edge in the $\text{Cd}_3(\text{As}_x\text{P}_{1-x})_2$ system is shown in Fig. 1. An approximately linear dependence of the edge on composition is observed for $x \leq 0.50$. For $x > 0.50$, a bowing is apparent which becomes more pronounced near the Cd_3As_2 end. Because of the high carrier concentrations, it is not immediately apparent whether the bowing is an intrinsic property of the system¹⁹ or primarily a result of the Burstein-Moss effect.

In order to analyze the transmission data an appropriate energy-band model is required. The electron effective mass in both Cd_3As_2 ^{8,10,11} and Cd_3P_2 ²⁰ is known to increase with carrier concentration. Since Lin-Chung's theoretical calculations also show^{15,16} that the system has a band structure similar to that of many III-V compounds, it is reasonable to assume a Kane model for the system as done by Wagner *et al.*³ and by others.^{10,11}

The model is shown schematically in Fig. 2 for positive and negative values of E_g , defined as the energy of band 1 minus that of band 3. For $E_g > 0$, the conduction band is *s* like and the three valence bands are *p* like. The lowest valence band is split

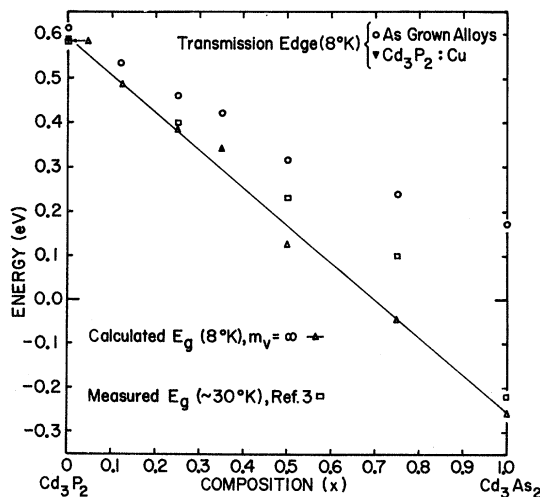


FIG. 1. Measured values of optical transmission edge and corresponding values of E_g from Eqs. (1)–(4). IMO data of Ref. 3 are included. The straight line is the best fit to the calculated points for $m_v = \infty$.

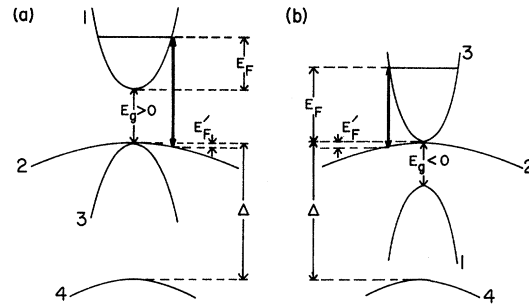


FIG. 2. Kane model proposed for $\text{Cd}_3(\text{As}_x\text{P}_{1-x})_2$ (after Wagner *et al.*, Ref. 3). (a) $E_g > 0$. As temperature increases, band 1 approaches band 2. (b) $E_g < 0$. As temperature increases, band 1 recedes from band 2. Heavy vertical lines indicate (direct) optical transitions.

off from the upper bands, which are degenerate at Γ , by the spin-orbit interaction. Of the two upper valence bands, only the lower-mass band (denoted band 3 in Fig. 2) interacts with the conduction band. This interaction increases with decreasing $|E_g|$, and there is an attendant decrease of the effective mass and the density of states at the bottom of the conduction band.

The transmission edge for direct transitions at 0°K may be defined as

$$E_{\text{opt}} = E_g + E_F(0) + E'_F(0), \quad E_g > 0$$

$$= E_F(0) + E'_F(0), \quad E_g < 0. \quad (1)$$

Here, $E_F(0)$ is the Fermi level at 0°K measured from the bottom of the conduction bands, and $E'_F(0)$ is defined as the difference between the valence-band energy at the Fermi wave vector and the energy at the top of the valence band (see Fig. 2). The Fermi energy for a band structure appropriate to the Kane model may be written as

$$E_F(0) = -\frac{1}{2} |E_g| + \frac{\hbar^2 k_F^2}{2m_0} + \frac{1}{2} \left(E_g^2 + \frac{4E_p \hbar^2 k_F^2}{3m_0} \right)^{1/2}, \quad (2)$$

where k_F is the Fermi momentum and E_p is a parameter related to the momentum matrix element p between bands 1 and 3 by $E_p = (2m_0/\hbar^2)p^2$. The other quantities have their customary meanings. Equation (2) neglects higher-band interactions and assumes that the spin-orbit interaction energy (Δ in Fig. 2) is large compared to E_g , as expected for $\text{Cd}_3(\text{As}_x\text{P}_{1-x})_2$.³ If the heavy-mass valence band is assumed to be approximately parabolic³ and characterized by a mass m_v , then

$$E'_F(0) = \hbar^2 k_F^2 / 2m_v. \quad (3)$$

Since the effective masses of Cd_3As_2 ⁸ and Cd_3P_2 ²⁰ are nearly isotropic, the Fermi momentum k_F may be reasonably approximated by

$$k_F^2 \approx (3\pi^2 N)^{2/3}, \quad (4)$$

where N is the carrier concentration. For the case of nondirect transitions originating from the top of the valence band, $E_{\text{opt}} = E_g + E_F(0)$. This result is formally equivalent to setting $m_v = \infty$ in Eq. (3).

Once N , E_p , and m_v are specified, the measured transmission edge E_{opt} uniquely determines E_g . The value of E_p in Cd_3P_2 is about 17 ± 2 eV.²⁰ As discussed above, however, there is considerable disparity in the values of E_p reported for Cd_3As_2 . Of the several reported measurements of E_p , the most reliable appear to be those of Armitage and Goldsmid¹⁰ and of Blom and Schrama¹¹ (18–19 eV). Since no measurements have been reported for any but the end-point alloys, E_p was assumed to be 18 eV for all values of x . This number is typical of those obtained for many III-V and II-VI compounds.

The carrier concentrations of the samples used in the present work were obtained from Hall measurements and are given in Table I. E_g was calculated for a series of values of m_v/m_0 between 0.2 and ∞ . For all choices of m_v an approximately linear variation of E_g with composition was obtained. The values closest to the IMO results were obtained for $E_F(0) = 0$ near the Cd_3As_2 end. The calculations are insensitive to m_v near the Cd_3P_2 end because of the much lower carrier concentrations in the phosphorus-rich alloys.

The low-temperature values of E_g (for $m_v = \infty$) are plotted in Fig. 1, in which the IMO results of Wagner *et al.*³ ($\approx 30^\circ\text{K}$) are also shown for comparison. There is some disagreement with the IMO gaps for $x = 0.50$ and $x = 0.75$, and therefore in the location of the crossover point. This discrepancy may arise from uncertainties in both measurements. The IMO gaps are difficult to estimate in the small-gap region,²¹ and the uncertainty in the present estimate of E_p (18 eV) has already been mentioned. The present calculation is also sensitive to errors in the carrier concentration for compositions close to the crossover point. Hall measurements of N are complicated by changes in the measured carrier concentration with temperature cycling and magnetic field.^{7,20} Consequently the quoted concentrations may be in error by 10% or more.

The availability of one Cd_3P_2 sample with low carrier concentration made it possible to observe directly the effect of the Burstein-Moss shift on the low-temperature transmission. The observed shift between the as-grown and copper-doped Cd_3P_2 samples (Fig. 1) is in good agreement with that calculated from Eqs. (2) and (3).

For the choice of $m_v = \infty$, the best straight-line fit to the low-temperature data for E_g as a function of composition is

$$E_g \text{ (eV)} = 0.588 - 0.834x. \quad (5)$$

The low-temperature electron effective mass at the Fermi level may be obtained by twice differen-

tiating Eq. (2) with respect to k_F . The result is

$$\frac{m^*}{m_0} \Big|_{T=0} = \left\{ 1 + \frac{2}{3} \left[\left(\frac{E_g}{E_p} \right)^2 + \frac{4\hbar^2 k_F^2}{3m_0 E_p} \right]^{-1/2} \right\}^{-1}. \quad (6)$$

The bottom-of-the-band mass is obtained by setting $k_F = 0$ in Eq. (6):

$$m_0^*/m_0 = (1 + 2E_p/3|E_g|)^{-1}. \quad (7)$$

Equation (7) may be readily evaluated for all x by substituting the value of 18 eV for E_p and using for E_g the values determined from Eq. (5). The results are given in Table I. The value of $m_0^*/m_0 = 0.014$ in Cd_3As_2 is in good agreement with that obtained (0.012) by other workers from thermomagnetic measurements on samples of different carrier concentrations.¹¹

B. Temperature Coefficient of Gap

In Fig. 3 the measured temperature dependence of the transmission edge is presented for each of the as-grown alloys; also included are data reported by other workers.^{3,12} The slopes of the curves are negative in all of the alloys and are approximately linear in the region above 100°K . At lower temperatures the magnitudes of the slopes decrease, as in many other materials. The values of the slopes in the linear region are plotted in Fig. 4. No systematic variation of the temperature coefficient with composition is apparent until corrections for the Fermi-level motion are made.

In the model of Fig. 2, the measured value of the temperature coefficient of the transmission edge may be regarded as stemming from two related effects: (a) the relative motion of bands 1 and 3 and (b) the consequent variation of the Fermi level.

$E_g > 0$. In the positive-gap regime,

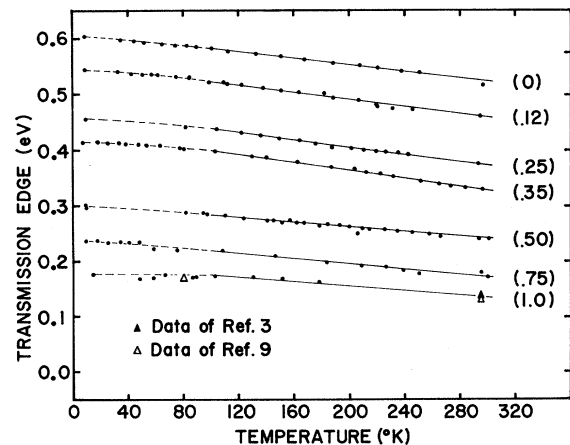


FIG. 3. Transmission edge for seven alloys between 8 and 300°K . Data of Refs. 3 and 12 are included. Numbers in parentheses are x values.

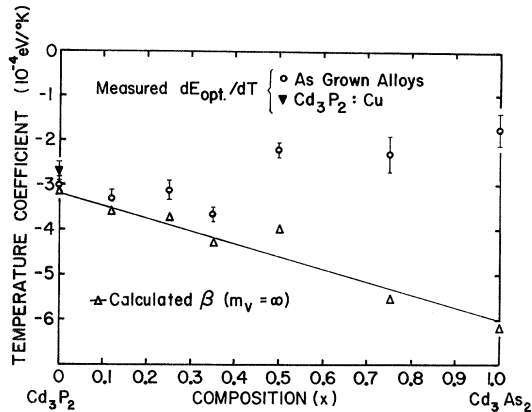


FIG. 4. Temperature coefficients of measured absorption edges and corresponding values of β from Eqs. (8) and (9). The straight line is the best fit to the calculated points for $m_v = \infty$.

$$\frac{dE_{\text{opt}}}{dT} = \beta + \frac{dE_F}{dT}, \quad (8)$$

where β is the rate of change with temperature of the difference in energy between bands 1 and 3. Since dE_{opt}/dT (and hence β) is observed to be negative, the bands approach each other with increasing temperature and the Fermi level increases [see Eq. (2)]. Thus dE_F/dT in Eq. (8) is positive. For large E_g and/or small N (e.g., in Cd_3P_2), this term is small.

$E_g < 0$. In this case,

$$\frac{dE_{\text{opt}}}{dT} = \frac{dE_F}{dT}. \quad (9)$$

The only effect of β is to vary E_F . Since dE_{opt}/dT is observed to remain negative through the crossover region, dE_F/dT must also be negative. This decrease of the Fermi level with temperature is brought about by a negative value of β . Thus bands 1 and 3 move in the same direction as a function of temperature, regardless of energy ordering.

The measured values of dE_{opt}/dT may be used to calculate β from Eqs. (2), (8), and (9). These calculated values of β are plotted in Fig. 4 for $m_v = \infty$. The result is an approximately linear dependence on composition from about -3×10^{-4} eV/°K in Cd_3P_2 to about -6×10^{-4} eV/°K in Cd_3As_2 . [It should be noted that the calculated values of β (Fig. 4) necessarily include contributions from lattice vibrations as well as lattice dilatation. The consequences of including the vibrational contribution to β are discussed at length in Sec. IV.]

In the calculation of the temperature coefficient three complicating effects have been neglected: free-carrier absorption, the variation of the Fermi level with temperature (apart from that due to changes in E_g), and the spreading of the Fermi dis-

tribution with temperature. Free-carrier absorption does not appreciably affect the location of the transmission edge in Cd_3As_2 ,¹² in which the absorption is at its strongest among the alloys.³ Hence this effect may be safely neglected. For degenerate samples with carrier concentrations comparable to those encountered here, the variation of the Fermi level with temperature is also negligible.²²

The effect of the spreading of the Fermi distribution on optical absorption in degenerate semiconductors has been treated by Kaiser and Fan.²³ Let α_0 be the absorption constant if the final state is unoccupied, and α the absorption constant in the degenerate material, at the same photon energy. If the conduction-band mass is much smaller than the valence-band mass, the transmission edge in the degenerate crystal is given by

$$h\nu(\alpha) = E_g + [E_F - kT \ln(\alpha_0/\alpha - 1)], \quad (10)$$

where the second term is the displacement of the edge with varying carrier concentration. Thus the earlier definition of the edge as $E_g + E_F$ (for $E_F' = 0$) will be in error by an amount proportional to kT . While this correction is negligible at helium temperatures, it may become appreciable at higher temperatures and can affect the measured value of the temperature coefficient. This effect is probably responsible for the observation that the measured value of dE_{opt}/dT in as-grown Cd_3P_2 ($N > 10^{17}$ cm⁻³) is greater than that in the copper-doped sample ($N < 10^{15}$ cm⁻³) by about 0.3×10^{-4} eV/°K (see Fig. 4).

It was not possible to analyze the absorption edges in these materials accurately enough to determine whether they are direct or indirect. However, there is independent evidence which suggests that while the Cd_3P_2 edge is direct,⁵ the Cd_3As_2 edge may be indirect.^{6,17} If this is indeed the case, then α_0 is probably smaller in Cd_3As_2 than in Cd_3P_2 . Consequently, the measured transmission edge in Cd_3As_2 should be shifted less than in Cd_3P_2 , and the calculated deviation in β for Cd_3P_2 , due to the broadening of the distribution function, is probably an upper limit for the system.

IV. DISCUSSION AND CONCLUSIONS

A. Low-Temperature Gaps

The proposal of a band crossing in the $\text{Cd}_3(\text{As}_x\text{P}_{1-x})_2$ alloy system near the Cd_3As_2 end, first offered by Wagner *et al.*,³ appears to be substantiated. Any choice of positive gap in Cd_3As_2 would raise the transmission edge to a higher photon energy than that observed in the $x = 0.75$ alloy. For no value of $E_g > 0$ is the sum of E_g and E_F less than 0.25 eV, whereas the observed edge occurs at 0.17 eV. Even if one assumes a 10% smaller carrier concentration and a value as low as 13 eV for E_p , the transmission edge should occur at a photon energy of 0.22 eV or higher for any positive value of E_g .

B. Temperature Coefficient

Although a direct comparison with experimental data is not feasible, it is nonetheless useful to write an approximate formula, based on the analysis of the temperature coefficient, for E_g as a function of composition between 100 and 300 °K:

$$E_g(\text{eV}) = 0.56 - (0.76 + 2.7 \times 10^{-4} T)x - 3.2 \times 10^{-4} T \quad (T \text{ in } ^\circ\text{K}). \quad (11)$$

As noted above, the measured values of dE_{opt}/dT , and therefore also the calculated values of β , include contributions from both lattice vibrations and lattice dilatation. It has been pointed out, however, that the Kane formulas are derived for a rigid lattice and hence take no account of the vibrational contribution to the energy gap.²⁴ Consequently it is incorrect, in general, to calculate effective masses from Eq. (6) at finite temperatures if the values of E_g given by Eq. (11) are used. The error should be totally negligible at helium temperatures, but discrepancies are known to arise between the calculated and measured effective masses of InSb at room temperature.²⁴ Ehrenreich²⁵ has introduced a parameter E_g^* , the effective-mass band gap, which satisfies Eq. (6) at all temperatures. Its exact relationship to E_g in Eq. (11) is not in general known, but Coderre and Woolley²⁶ have shown that E_g^* is appreciably greater than E_g in InAs_xSb_{1-x} alloys at high temperatures.

Among the Cd₃(As_xP_{1-x})₂ alloys, only in Cd₃As₂ has the effective mass been measured as a function of temperature^{7,27} so as to afford a means of comparing E_g and E_g^* and of estimating thereby the magnitude of the vibrational contribution to β . The experimental masses⁷ are given in Table II along with the masses calculated from Eqs. (6) and (11) for Cd₃As₂ at liquid-nitrogen and room temperatures. It is significant first that the calculated values exhibit the correct temperature dependence. In the model of Fig. 2(b), as bands 1 and 3 move apart with increasing temperature, the mass at the Fermi level increases. If a positive-gap model were appropriate for Cd₃As₂, the mass at the Fermi level would decrease with increasing temperature.

Although the calculated masses are systematically higher than the experimental values in Table II, the percentage changes in the calculated effective masses as a function of temperature, for both values of N , do not differ greatly from the experiment-

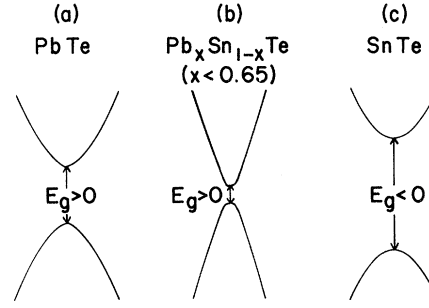


FIG. 5. Two-band model of Pb_xSn_{1-x}Te (after Dimmock *et al.*, Ref. 30). (a) $x=1$, $E_g > 0$. As temperature increases, bands approach each other. (b) $x < 0.65$, $E_g > 0$. (c) $x=0$, $E_g < 0$. As temperature increases, bands separate.

ally observed change. Consequently E_g^* and E_g differ also by only a small amount. While the accuracy of the calculations and of the experimental data probably does not warrant a more quantitative comparison, it may safely be concluded that the dilatational contribution to β is larger than the vibrational contribution. This conclusion may be verified by calculating the vibrational contribution. For optical model scattering, which appears to be the dominant mechanism in Cd₃As₂,^{10,28} the vibrational contribution is²⁹

$$\beta_{\text{vib}} = -\sqrt{2} \pi e^4 k \hbar (m^*)^{1/2} / (\hbar \nu)^{5/2} a^3 M. \quad (12)$$

Here, ν is the frequency of optical phonons, a is the interionic spacing, and M is the reduced ionic mass. Evaluation of Eq. (12) yields $\beta_{\text{vib}} \approx -1 \times 10^{-4}$ eV/°K, which is small by comparison with the calculated value of $\beta = -6 \times 10^{-4}$ eV/°K.

The discrepancy between corresponding values of calculated and measured effective masses in Table II is due in part to the uncertainty in the experimental value of N ²⁸ and also to the uncertainty in the choice of E_p . Increasing E_p and decreasing N yield somewhat smaller masses but do not appreciably affect the calculated percentage increase of the effective mass with temperature.

Another band model which was considered as a possible description of Cd₃(As_xP_{1-x})₂ is that proposed by Dimmock *et al.*³⁰ for Pb_xSn_{1-x}Te. The sign of the temperature coefficient is of value in distinguishing this model from the Kane model described above. In the Pb_xSn_{1-x}Te system (Fig. 5) the conduction and valence bands of PbTe approach each other with in-

TABLE II. Measured and calculated electron effective masses in Cd₃As₂.

Temperature (°K)	Calculated m^*/m_0		Experimental m^*/m_0 (Ref. 7) $N \approx 2 \times 10^{18} \text{ cm}^{-3}$
	$N = 1.5 \times 10^{18} \text{ cm}^{-3}$	$N = 2.0 \times 10^{18} \text{ cm}^{-3}$	
78	0.043	0.047	0.042
300	0.048	0.051	0.045

creasing Sn concentration and eventually exchange roles. The temperature dependence of the optical transmission edge is given by

$$\frac{dE_{\text{opt}}}{dT} = \frac{d|E_g|}{dT} + \frac{dE_F}{dT}. \quad (13)$$

For this system, E_g , which is defined as the energy of band 1 minus the energy of band 2, is taken to be positive in PbTe and negative in SnTe (see Fig. 5). For carrier concentrations less than $7 \times 10^{19} \text{ cm}^{-3}$, the first term in Eq. (12) changes sign when E_g changes sign ($x \approx 0.65$ at 12°K), since the motion of the bands as a function of temperature is independent of energy ordering.^{30,31} The measured value of dE_{opt}/dT also changes sign³⁰ because the first term is dominant. This result is opposite to that deduced above for the Kane model, in which the

temperature coefficient does not change sign when E_g passes through zero. The observation that a negative temperature coefficient persists throughout the $\text{Cd}_3(\text{As}_x\text{P}_{1-x})_2$ series thus serves to exclude the $\text{Pb}_x\text{Sn}_{1-x}\text{Te}$ model.

ACKNOWLEDGMENTS

We should like to thank E. M. Swiggard, P. G. Siebenmann, and Dr. M. W. Heller for providing the crystals and the results of transport measurements prior to publication, and J. M. Chaney for assistance in sample preparation. We are indebted to Dr. B. D. McCombe, Dr. R. J. Wagner, Dr. E. D. Palik, Dr. S. Teitler, and Dr. J. D. Wiley for many illuminating discussions and for assistance in preparing the manuscript.

*Supported in part by Naval Electronics Systems Command.

¹S. G. Bishop, W. J. Moore, and E. M. Swiggard, *Appl. Phys. Letters* **15**, 12 (1969).

²S. G. Bishop, W. J. Moore, and E. M. Swiggard, in *Proceedings of the Third International Conference on Photoconductivity, Stanford University, 1969*, edited by F. M. Pell (Pergamon, Oxford, 1971), p. 205.

³R. J. Wagner, E. D. Palik, and E. M. Swiggard, *J. Phys. Chem. Solids Suppl.* **1**, 471 (1971).

⁴W. Zdanowicz and A. Wojakowski, *Phys. Status Solidi* **8**, 569 (1965).

⁵S. G. Bishop, W. J. Moore, and E. M. Swiggard, *Appl. Phys. Letters* **16**, 459 (1970).

⁶L. Zdanowicz, *Phys. Status Solidi* **20**, 473 (1967).

⁷E. D. Haidemenakis, M. Balkanski, E. D. Palik, and J. Tavernier, *J. Phys. Soc. Japan Suppl.* **21**, 189 (1966).

⁸I. Rosenman, *J. Phys. Chem. Solids* **30**, 1385 (1969).

⁹E. O. Kane, in *Semiconductors and Semimetals*, edited by R. K. Willardson and A. C. Beer (Academic, New York, 1966), pp. 75-100.

¹⁰D. Armitage and H. J. Goldsmid, *J. Phys. C* **2**, 2389 (1969).

¹¹F. A. P. Blom and J. Th. Schrama, *Phys. Letters* **30A**, 245 (1969).

¹²W. J. Turner, A. S. Fischler, and W. E. Reese, *J. Appl. Phys. Suppl.* **32**, 2241 (1961).

¹³S. H. Groves, R. M. Brown, and C. R. Pidgeon, *Phys. Rev.* **161**, 779 (1967).

¹⁴S. H. Groves and W. Paul, *Phys. Rev. Letters* **11**,

194 (1963).

¹⁵P. J. Lin-Chung, *Phys. Rev.* **188**, 1271 (1969).

¹⁶P. J. Lin-Chung (private communication).

¹⁷S. G. Bishop and P. L. Radoff, *Solid State Commun.* **9**, 133 (1971).

¹⁸G. Haacke and G. A. Castellion, *J. Appl. Phys.* **35**, 2484 (1964).

¹⁹J. A. Van Vechten and T. K. Bergstresser, *Phys. Rev. B* **1**, 3351 (1970).

²⁰M. W. Heller, J. Babiskin, E. M. Swiggard, and P. L. Radoff, *Bull. Am. Phys. Soc.* **16**, 370 (1971).

²¹R. J. Wagner (private communication).

²²J. S. Blakemore, *Semiconductor Statistics* (Pergamon, New York, 1962), p. 84.

²³W. Kaiser and H. Y. Fan, *Phys. Rev.* **98**, 966 (1955).

²⁴E. D. Palik, G. S. Picus, S. Teitler, and R. F. Wallis, *Phys. Rev.* **122**, 475 (1961).

²⁵H. Ehrenreich, *J. Phys. Chem. Solids* **2**, 131 (1957).

²⁶W. M. Coderre and J. C. Woolley, *J. Phys. Chem. Solids Suppl.* **1**, 535 (1971).

²⁷F. A. P. Blom and A. Huyser, *Solid State Commun.* **7**, 1299 (1969).

²⁸M. W. Heller (private communication).

²⁹H. Y. Fan, *Phys. Rev.* **82**, 900 (1951); *Rept. Progr. Phys.* **19**, 107 (1956).

³⁰J. A. Dimmock, I. Melngailis, and A. J. Strauss, *Phys. Rev. Letters* **16**, 1193 (1966).

³¹Y. W. Tsang and Marvin L. Cohen, *Phys. Rev. B* **3**, 1254 (1971).